<div align="center">

Supporting Information:
The role of methyl–induced polarization in ion binding

Mariana Rossi, Alexandre Tkatchenko, Susan B. Rempe and Sameer Varma

June 26, 2013

</div>

In Table S1, the computational estimates are obtained as follows. The reactant and product molecular configurations are first relaxed separately at the PBE+vdW level of theory [1], using the all-electron program package FHI-aims [2]. We used *tight* settings for the numeric atom centered orbitals basis sets and integration grids, as explained in Ref. [2]. Following relaxation, the complex geometries are subjected to a single point calculation using the hybrid PBE0[3, 4]+vdW functional, which yields their electronic energies E. The Gibbs free energy of each complex is then estimated using the ideal gas thermodynamic relationship, $G = F + k_B T$, where k_B is the Boltzmann constant, $T = 298$ K, and F is the Helmholtz free energy. Assuming that the coupling between translational, vibrational and rotational degrees of freedom can be neglected, F is estimated as a sum of their independent contributions [5], that is, $F = F_{trans} + F_{vib} + F_{rot}$, where

$$F_{trans} = -k_B T \left[\ln \left(\frac{m k_B T}{2\pi \hbar^2} \right)^{3/2} + \ln \frac{k_B T}{P} + 1 \right],$$

$$F_{vib} = E + \sum_{i}^{3N-6} \left[\frac{\hbar \omega_i}{2} + k_B T \ln \left(1 - \exp^{-\frac{\hbar \omega_i}{k_B T}} \right) \right], \text{ and}$$

$$F_{rot} = -\frac{3}{2} k_B T \ln \left[\frac{2 k_B T}{\hbar^2} (I_A I_B I_C)^{1/3} \pi^{1/3} \right].$$

In the expressions above, N is the number of atoms in the molecule, I_A, I_B, and I_C are the molecular moments of inertia, $P = 1$ atmosphere, m is the molecular mass and ω_i are the harmonic vibrational frequencies obtained from a Hessian analysis of the PBE+vdW energy surface. The reaction free energy changes ΔG are then obtained by subtracting the free energies of reactant complexes from the product complexes; that is, $\Delta G = \sum n_p G_p - \sum n_r G_r$, where n_p and n_r are the stoichiometries of the products and reactants. *We find that computed values agree with experiments.* The inclusion of dispersion van der Waals interactions is crucial, as shown by the amount of dispersion energy, $\Delta E_{vdW} = \Delta E_{\text{PBE0}+vdW} - \Delta E_{\text{PBE0}}$, in each computed reaction free energy change in Table S1.

Table S1: Comparison between experimental and computed reaction free energy changes ΔG involving Na^+, K^+ and Ba^{2+} ions forming complexes with water (W) and methanol (M) molecules. ΔE_{vdW} is the contribution of dispersion energy to the computed ΔG. All energies are in units of kcal/mol.

Gas phase reaction	Experiment	Theory	
	ΔG	ΔG^a	ΔE_{vdW}
$Na + W \rightleftharpoons NaW$	-18.8[b]	-17.6	-0.3
$Na + 2W \rightleftharpoons NaW_2$	-31.9[b]	-32.1	-0.8
$Na + 3W \rightleftharpoons NaW_3$	-40.9[b]	-42.2	-1.7
$Na + 2M \rightleftharpoons NaM_2$	-35.5[c]	-35.6	-2.0
$Na + 3M \rightleftharpoons NaM_3$	-44.7[c]	-46.2	-4.8
$K + W \rightleftharpoons KW$	-11.8[b]	-11.8	-0.7
$K + 2W \rightleftharpoons KW_2$	-20.7[b]	-22.9	-1.4
$K + 3W \rightleftharpoons KW_3$	-27.0[b]	-28.6	-2.1
$K + M \rightleftharpoons KM$	-13.4[d]	-13.7	-1.0
$K + 2M \rightleftharpoons KM_2$	-23.1[e]	-23.8	-3.3
$K + 3M \rightleftharpoons KM_3$	-29.9[e]	-29.3	-5.9
$BaW_4 + W \rightleftharpoons BaW_5$	-16.1[f]	-14.6	-1.0
$BaW_5 + W \rightleftharpoons BaW_6$	-12.6[f]	-14.0	-0.9

[a] Computed at T=298 K, except for the reaction $K + M \rightleftharpoons KM$, whose free energy was computed at T=443 K. [b] Estimated at T=298 K and taken from reference [6]. [c] Estimated by adding $NaW_n + nM \rightleftharpoons NaM_n + nW$ substitution reaction free energies obtained at T=303 K [7] to corresponding NaW_n complexation energies obtained at T=298 K [6]. [d] Estimated by adding the $KW + M \rightleftharpoons KM + W$ reaction free energy obtained at T=443 K to the KW complexation energy taken from reference [7]. [e] Estimated by adding $KW_n + nM \rightleftharpoons KM_n + nW$ substitution reaction free energies obtained at T=302 K [7] to corresponding KW_n complexation energies obtained at T=298 K [6]. [f] Estimated at T=298 K and taken from reference [8].
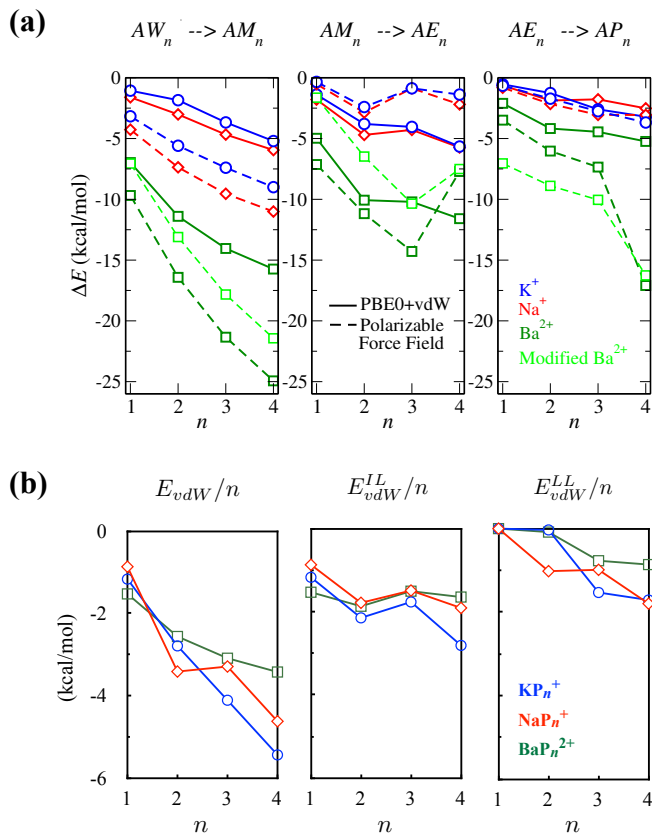
Figure S1: (a) Comparison of substitution reaction energy changes (ΔE) obtained from PBE0+vdW [1] and a polarizable force field [9, 10, 11]. ΔE are estimated for the substitution reactions studied in Figure 2 of the main manuscript, and are computed using geometries relaxed separately at the respective levels of theory. Geometry relaxations employing PBE0+vdW are carried out using FHI-AIMS [2] as described in the methods section of the main manuscript, and relaxations employing the polarizable force field are carried out using the optimize algorithm of TINKER v6.2 with a RMS gradient cut off of 0.01 kcal/mol. Note that we utilize two separate parameter sets for Ba^{2+}, one taken from [12], and the other (Ba^{2+} modified) in which we reduced the Ba^{2+} damping factor five–fold from 0.39 to 0.078, as suggested in references [13, 14]. We find that while a polarizable force field can reproduce the PBE0+vdW trends, the quantitative differences can be large. (b) To understand the origin of these differences we examine one specific energetic contribution that is not modeled explicitly in the polarizable force field. The atomic C_6 dispersion coefficients are kept fixed in the polarizable force field. In contrast, the C_6 coefficients are variables in the PBE0+vdW method that depend on self–consistent electron densities. For example in the ion–propanol complexes, we find that the C_6 coefficients of Na^+, K^+, and Ba^{2+} vary by factors of $\sim$8, $\sim$5 and $\sim$3, respectively. To understand the energetic consequences of such variations in C_6 coefficients in ion–propanol complexes, we divide the total dispersion energy (E_{vdW}) into intra–ligand (E_{vdW}^L), ligand–ligand (E_{vdW}^{LL}), and ion–ligand (E_{vdW}^{IL}) contributions. We define for a given geometry AP_n, $E_{vdW}(AP_n) = E_{\text{PBE0}+vdW}(AP_n) - E_{\text{PBE0}}(AP_n)$, $E_{vdW}^L(AP_n) = n \times (E_{\text{PBE0}+vdW}(P) - E_{\text{PBE0}}(P))$, $E_{vdW}^{LL}(AP_n) = E_{\text{PBE0}+vdW}(P_n) - E_{\text{PBE0}}(P_n) - E_{vdW}^L(AP_n)$ and $E_{vdW}^{IL}(AP_n) = E_{vdW}(AP_n) - E_{vdW}^{LL}(AP_n) - E_{vdW}^L(AP_n)$. We find that E_{vdW}^{IL} increases non–linearly with the number of propanols in the complex, and, in fact, the E_{vdW}^{IL} are correlated strongly with the ion C_6 coefficients (Pearson correlations > 0.96). This suggests that the differences between PBE0+vdW and the polarizable force field can emerge from the differences in the descriptions of dispersion interactions. The convergence with PBE0+vdW may be improved by introducing C_6 coefficient variability in polarizable fields.
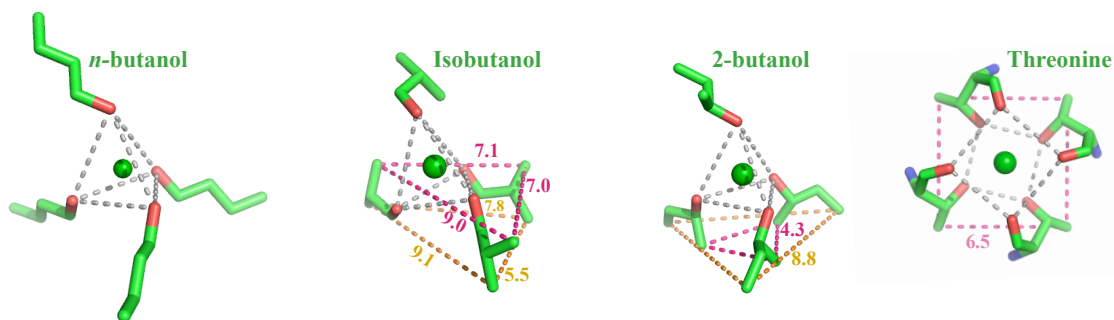
Figure S2: Optimized configurations of representative 4-fold butanol complexes compared with the S4 site. The central ion in each case is Ba^{2+}. The dashed lines serve as visual aids. The grey lines indicate the coordination geometry, and the magenta/orange lines indicate the distances between the branched methyl groups of adjacent ligands. All distances are in Ångstrom units. We note that the packing of the branched methyl group of threonine in the S4 site of KcsA is intermediate between the packing of branched methyl groups in 4-fold complexes comprised of 2-butanols and isobutanols

Table S2: Effect of $T \to S$ substitutions on the structures of ion complexes. In the calculation of the root mean squared deviation (RMSD) between two ion-complexes, only non-hydrogen atoms are considered. Note that two simultaneous $T \to S$ substitutions can be introduced in two different ways. In one case, the substitutions can be made on adjacent threonine residues, and in the other case, the substitutions are made on non-adjacent threonine residues. The numbers in brackets correspond to substitutions made on adjacent threonine residues. We find that these substitutions result in only minor configurational changes. While the configurational changes are generally higher in the case of Ba^{2+} complexes, they do not correspond to any changes in binding topology or geometry (see Figure S3).

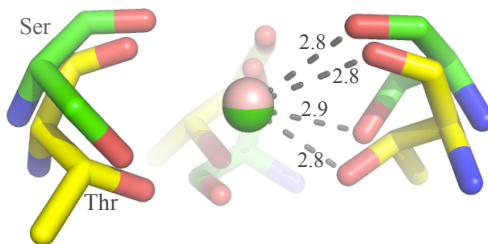| RMSD (in Å) between	A ≡ Na^+	A ≡ K^+	A ≡ Ba^{2+}
AT_4 & AT_3S	0.13	0.46	0.85
AT_4 & AT_2S_2	0.13 (0.14)	0.69 (0.02)	0.84 (0.96)
AT_4 & AT_1S_3	0.14	0.64	0.96
AT_4 & AS_4	0.03	0.02	1.01

Figure S3: Superimposed optimized configurations of the BaT_4 and BaS_4 complexes. While the RMSD between the two optimized configurations is 1.01 Å, their coordination geometries are the same. Note that only three out of the four bidentate ligands in the complexes are shown. The distances between the coordinating oxygen atoms and ions are in Ångstroms.

Table S3: Changes in single point energy ΔE and free energy ΔG associated with the substitution reaction, $BaT_4 + 4S \rightleftharpoons BaS_4 + 4T$, estimated with and without vdW contributions. The vdW contributions are evaluated in two different ways: (1) using a pairwise approximation [1], denoted by PBE0+vdW, and (2) using a many-body correction scheme [15], denoted by PBE0+mbd. Free energies are evaluated at a temperature of 298 K and a pressure of 1 atmosphere. All energies are in units of kcal/mol. We find that while the contributions of many-body vdW interaction terms to ΔE are small (0.3 kcal/mol), dispersion contributes significantly to the energy differences associated with the substitution reaction.

	PBE0	PBE0+vdW	PBE0+mbd
$\Delta E = E_{BaS_4} + 4E_T - E_{BaT_4} - 4E_S$	3.1	5.2	4.9
$\Delta G = G_{BaS_4} + 4G_T - G_{BaT_4} - 4G_S$	2.5	6.9	-

References

[1] A. Tkatchenko and M. Scheffler. Accurate molecular van der Waals interactions from ground-state electron density and free-atom reference data. *Phys. Rev. Lett.*, 102:073005, 2009.

[2] V Blum, R Gehrke, F Hanke, P Havu, X Ren, K Reuter, and M Scheffler. Ab initio molecular simulations with numeric atom-centered orbitals. *Comp. Phys. Comm.*, 180:2175–2196, 2009.

[3] M. Ernzerhof and G. E. Scuseria. Assessment of the Perdew-Burke-Ernzerhof exchange-correlation functional. *J Chem. Phys.*, 110:5029, 1999.

[4] C. Adamo and V. Barone. Toward reliable density functional methods without adjustable parameters: The pbe0 model. *J Chem. Phys.*, 110(13):6158–6170, 1999.

[5] Donald McQuarrie. *Statistical Mechanics*. University Science Books, 1st edition, 2000.

[6] MD Tissandier *et al.* The proton's absolute aqueous enthalpy and Gibbs free energy of solvation from cluster-ion solvation data. *J. Phys. Chem. A*, 102:7787–7794, 1998.

[7] S.B. Nielsen, M Masella, and P Kebarle. Competitive gas-phase solvation of alkali metal ions by water and methanol. *J. Phys. Chem. A*, 103:9891–9898, 1999.

[8] M. Peschke, AT Blades, and P Kebarle. Hydration energies and entropies for Mg^{2+}, Ca^{2+}, Sr^{2+}, and Ba^{2+} from gas-phase ion-water molecule equilibria determinations. *J. Phys. Chem. A*, 102:9978–9985, 1998.

[9] P Ren, and JW Ponder. Polarizable Atomic Multipole Water Model for Molecular Mechanics Simulation. *J. Phys. Chem. B*, 107:5933–5947, 2003.

[10] A Grossfield, P Ren, and JW Ponder. Ion Solvation Thermodynamics from Simulation with a Polarizable Force Field. *J. Amer. Chem. Soc.*, 125:15671–15682, 2003.

[11] P Ren, C Wu, and JW Ponder Polarizable Atomic Multipole-Based Molecular Mechanics for Organic Molecules. *J Chem. Theor. Comput.*, 7:3143–3161, 2011.

[12] TINKER – Software Tools for Molecular Design Version 4.3. (http://dasher.wustl.edu/ffe/downloads/)

[13] JP Piquemal, L Perera, GA Cisneros, P Ren, LG Pedersen, and TA Darden Towards accurate solvation dynamics of divalent cations in water using the polarizable amoeba force field: From energetics to structure *J. Chem. Phys.*, 125: 054511, 2006.

[14] JW Ponder, C Wu, P Ren, VS Pande, JD Chodera, MJ Schnieders, I Haque, DL Mobley, DS Lambrecht, RA DiStasio, Jr., M Head-Gordon, GNI Clark, ME Johnson, and T Head-Gordon Current Status of the AMOEBA Polarizable Force Field *J. Phys. Chem. B*, 114:2549–2564, 2010.

[15] A. Tkatchenko, R.A. DiStasio, R. Car, and M. Scheffler. Accurate and efficient method for many-body van der Waals interactions. *Phys. Rev. Lett.*, 108:236402, 2012.